catalysts

MDPI

Article

Synthesis of (*S*)- and (*R*)-β-Tyrosine by Redesigned Phenylalanine Aminomutase

Fei Peng, Habibu Aliyu, André Delavault, Ulrike Engel and Jens Rudat *

Technical Biology, Institute of Process Engineering in Life Sciences, Karlsruhe Institute of Technology, Fritz-Haber-Weg 4, 76131 Karlsruhe, Germany; fei.peng@kit.edu (F.P.); habibu.aliyu@kit.edu (H.A.); andre.delavault@kit.edu (A.D.); ulrike.engel@kit.edu (U.E.)
* Correspondence: jens.rudat@kit.edu; Tel.: +49-721-608-48428

Abstract: Phenylalanine aminomutase from *Taxus chinensis* (TchPAM) is employed in the biosynthesis of the widely used antitumor drug paclitaxel. TchPAM has received substantial attention due to its strict enantioselectivity towards (*R*)-β-phenylalanine, in contrast to the bacterial enzymes classified as EC 5.4.3.11 which are (*S*)-selective for this substrate. However, the understanding of the isomerization mechanism of the reorientation and rearrangement reactions in TchPAM might support and promote further research on expanding the scope of the substrate and thus the establishment of large-scale production of potential synthesis for drug development. Upon conservation analysis, computational simulation, and mutagenesis experiments, we report a mutant from TchPAM, which can catalyze the amination reaction of *trans-p*-hydroxycinnamic acid to (*R*)- and (*S*)-β-tyrosine. We propose a mechanism for the function of the highly conserved residues L179, N458, and Q459 in the active site of TchPAM. This work highlights the importance of the hydrophobic residues in the active site, including the residues L104, L108, and I431, for maintaining the strict enantioselectivity of TchPAM, and the importance of these residues for substrate specificity and activation by altering the substrate binding position or varying the location of neighboring residues. Furthermore, an explanation of (*R*)-selectivity in TchPAM is proposed based on the mutagenesis study of these hydrophobic residues. In summary, these studies support the future exploitation of the rational engineering of corresponding enzymes with MIO moiety (3,5-dihydro-5-methylidene-4H-imidazole-4-one) such as ammonia lyases and aminomutases of aromatic amino acids.

Keywords: enantioselectivity; β-amino acid; computational enzyme design; functional residues TchPAM; phenylalanine aminomutase

Citation: Peng, F.; Aliyu, H.; Delavault, A.; Engel, U.; Rudat, J. Synthesis of (*S*)- and (*R*)-β-Tyrosine by Redesigned Phenylalanine Aminomutase. *Catalysts* **2022**, *12*, 397. https://doi.org/10.3390/catal12040397

Academic Editor: Evangelos Topakas

Received: 7 March 2022
Accepted: 30 March 2022
Published: 1 April 2022

1. Introduction

Optically pure β-amino acids, representing fundamental building blocks in pharmaceutical and agrochemical products, have achieved growing attention in the field of medicinal application due to their antibacterial and anticancer properties [1–3]. In contrast to the proteinogenic α-amino acids, β-amino acids can be used to prepare prodrugs with a high stability against proteolytic degradation. One clinical and commercially successful example of a β-amino acid-containing drug is paclitaxel (Taxol®), an antimicrotubule drug for the treatment of various leukemias and solid tumors, which was first isolated from the *Taxus* species [4]. Paclitaxel, harboring a modified β-phenylalanine moiety (Figure 1), exerts its antitumor activity by interfering with cellular cycling through the stabilization of microtubules [5,6].

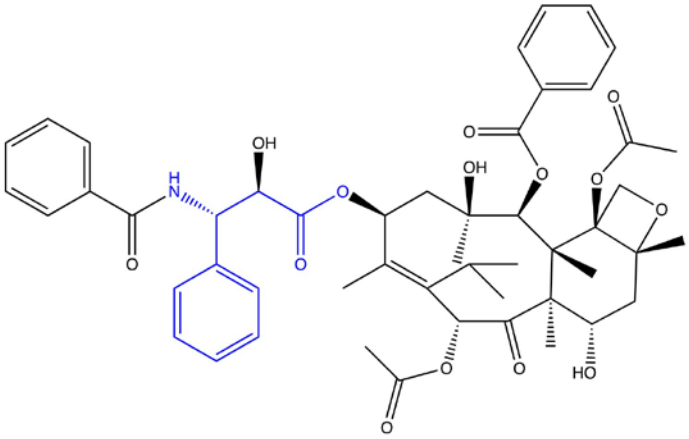

Figure 1. The structure of (*2R,3S*)-phenylisoserine is an essential part of the antitumor drug Paclitaxel (Taxol®). The natural synthesis of this non-canonical amino acid starts with the enzymatic isomerization of L-α-phenylalanine to (*R*)-β-phenylalanine by an aminomutase. A subsequent hydroxylation at the α-carbon changes the absolute configuration of the β-carbon from (*S*) to (*R*) [7].

The chemical synthesis processes of β-amino acids have been well-established over the past few decades [1,3]. However, these chemical industries are limited in enantioselectivity and currently face problems of environmental pollution, leading to the development of cleaner and economic strategies for β-amino acid production based on enzymatic conversion. Compared to chemical synthesis processes, the generation of β-amino acids by enzymatic conversion produces less chemical waste because of the fewer intermediary reaction steps [8]. Concerning the enantioselectivity, the aromatic ammonia-lyase and aminomutase are efficient enzymes without cofactor recycling. These enzymes, which are employed for the conversion of L-histidine, L-phenylalanine, or L-tyrosine to give corresponding α, β-unsaturated acids, have been classified in the MIO (3,5-dihydro-5-methylidene-4H-imidazole-4-one)-dependent enzyme family, since they share the identical catalytic mechanism and structures with an electrophilic MIO prosthetic group [9]. The MIO moiety, which was first observed in the crystal structure of PpHAL from *Pseudomonas putida*, is spontaneously formed by the tripeptide Ala142-Ser143-Gly144 when the protein folds in the late stage [10,11]. The formation mechanism has been proposed based on the well-known post-translational modifications in green fluorescent protein from *Aequorea victoria* (AvGFP) [12]. The initial cyclization step, involving a nucleophilic attack of the amide nitrogen of a glycine (Gly67 in AvGFP, Gly144 in PpHAL, and Gly177 in TchPAM) on the carbonyl oxygen of amino acid (Ser65 in AvGFP, Ala142 in PpHAL, and Ala175 in TchPAM), is quite similar in both MIO-dependent enzymes and GFP. The following mutagenesis and molecular simulation studies on PpHAL highlight the importance of neighboring residues and water molecules for electronically unfavorable cyclization. Among them, the residue Asn195 was conformed to activate the reacting amides by forming the hydrogen bond, while the other residue Asp145 provides the mechanical compression for the cyclization of the loop. In PpHAL, the residues Glu414 and Tyr280 form a hydrogen-bonding network with the residue Ser143, promoting a subsequent exocyclic dehydration reaction (Figure 2) [13].

The MIO prosthetic group promotes an addition reaction with the α-amine of the substrate [14]. Then, the pro-*S*-proton at β-position is abstracted by a catalytic essential base Tyr80, which is located on the inner loop that influences the enzyme activity by conformation switching [15,16]. Following this deprotonation step, the MIO–amine leaves from the generated carbanion intermediate, releasing the unsaturated acid as the product. The carbanion intermediate can be stabilized by the surrounding residues with a functional side chain in the enzyme. The enhanced stability of the intermediate leads to a favorable E1cB-elimination reaction, which is common in biology [14]. To prepare the free enzyme

for the next catalytic cycle, the alkene on MIO prosthetic group is rebuilt by the elimination of ammonia [14].

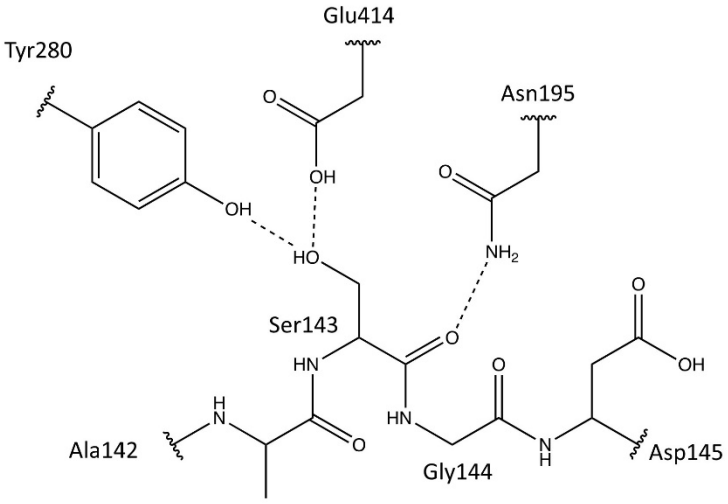

Figure 2. The tripeptide Ala-Ser-Gly in PpHAL and the residues involving the cyclization and dehydration of the loop.

TchPAM, a unique member of the MIO-dependent enzyme family, can catalyze both the ammonia addition of *trans*-cinnamic acids and the rearrangement of (*S*)-α-phenylalanine to yield (*R*)-β-phenylalanine with a high enantiopurity. According to the proposed isomerization mechanisms in the earlier studies on phenylalanine aminomutase, two readdition pathways could be assumed when (*S*)-α-tyrosine is bound with the carboxyl group in the active site as the substrate. The rotation of the C-C bond might occur only if the β-position of the intermediate is located too far from the NH_2-MIO, leading to an ammonia readdition on the opposite face. Otherwise, the amine-MIO adduct could rebind on unsaturated acids immediately, yielding the (*S*)-β-tyrosine as the main product [17–20].

2. Results and Discussion

Following the earlier X-ray crystallographic studies on TchPAM, the major residues surrounding the bound substrate are essential for MIO moiety formation (Ala175, Ser176, Gly177, Asp178, and Tyr322), catalytic activation (Tyr80), substrate binding (Asn231, Gln319, Arg325, and Asn355 in the carboxyl binding pocket and Phe86, Leu104, and Ile431 in the aromatic binding pocket), and the sterically constraining neighboring residues (Tyr424, Lys427, and Glu455) [17,20,21] (Figure 3) [22]. However, the function of the other residues within a 9 Å sphere of the bound ligand remains unclear.

In theory, the functional and structural constraints limit the spontaneous mutation of the catalytically essential residues, while the substrate-binding residues can mutate to the amino acids with similar properties [23]. Therefore, the conservation of these residues was initially determined by performing a multiple-sequence alignment with PAM and homologues, including the SwissProt-collected PAL, TAL, TAM, and HAL. As shown in Figure 4B, apart from the residues involved in the catalysis or MIO moiety formation, the residues Leu179, Leu227, Gly368, Phe371, Asn458, and Gln459 were also highly conserved in the enzymes, which could catalyze the cinnamic acid and produce the phenylalanine. Conversely, the residues Asn458 and Gln459 were replaced by the amino acids with similar characteristics in the other members from the MIO-dependent enzyme family (Figure 4A). These results suggest that the residues Asn458 and GLn459 might change the substrate selectivity but may not affect the formation of the electrophilic prosthetic group in the active site. Similarly, Leu104, Lys427, Ile431, and Glu455 from the binding site could be considered as the important residues for substrate selectivity.

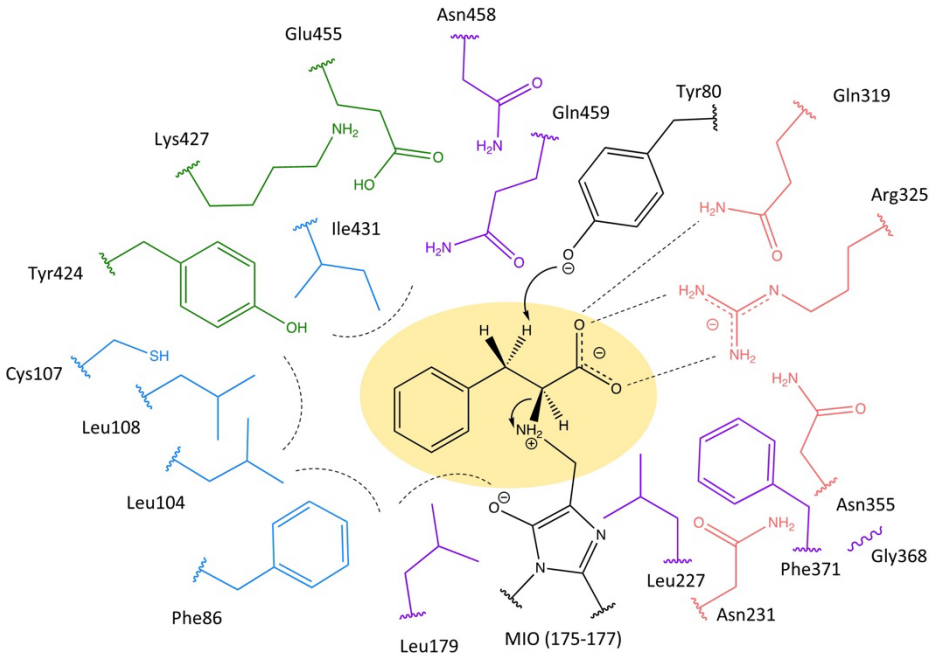

Figure 3. Schematic representation of the active site residues, which were located within 9 Å of the ligand (e.g., phenylalanine, which is highlighted by the yellow background) in the active site of TchPAM. The color coding corresponds to the function of the residues: activation (black), carboxyl binding pocket (red), aromatic binding pocket (blue), steric or electronic effects on the residues in the aromatic binding pocket (green), highly conserved residues (purple).

2.1. Highly Conserved Residues

Subsequently, the residues Leu227, Gly368, Phe371, Asn458, and Gln459 were mutated without any limitation for docking with β-tyrosine using PyRosetta. The designed variants with low scores were chosen for experimental characterization after calculation with PyRosetta, involving the ligand binding energy, the catalytic constraint score, and the total score. For an investigation of the substrate tolerance, the selected mutants and the wild type were reacted with (*S*)-α-phenylalanine, (*R*)-β-phenylalanine, (*S*)-α-tyrosine, and (*R*)-β-tyrosine. The variation of residues Leu227, Gly368, and Phe371 were not observed in over 1000 designed results, which was consistent with their strict conservation. As shown in Figure 5, some variations of the residues Leu179, Asn458, and Gln459 still had the ability to accept phenylalanine as a substrate, albeit with considerably lower activity. Except for the mutant Gln459Cys, the other mutants lost the catalytic activity for tyrosine.

The X-ray crystallographic study of the mutant Asp145Ala on PpHAL from *Pseudomonas putida* revealed the existence of a mechanical compression by residue Asp145 (Asp178 in TchPAM) against the reacting loop during the cyclization of the MIO moiety, which was strongly supported by the further molecular dynamics simulation of the active site in PpHAL with the hybrid quantum mechanics/molecular mechanics calculation (QM/MM) [11,13]. From a similar point of view, the highly conserved residue Leu179, located in close contact with the residue MIO prosthetic group (Ala175-Gly177), could be assumed to occupy an important position for moiety formation. However, when the residue Leu179 was mutated to the residue with a polar side chain, the mutant Leu179Thr exhibited 16% ammonia–lyase activity to (*R*)-β-phenylalanine, suggesting that this residue was not strictly required to press the MIO loop for proper protein folding but might act as a substrate-binding residue due to its hydrophobicity. The polar side chain on this residue could change the position of the phenolic ring on the substrate, which was supported by the lack of activity for tyrosine in mutants Leu179Ser and Leu179Thr.

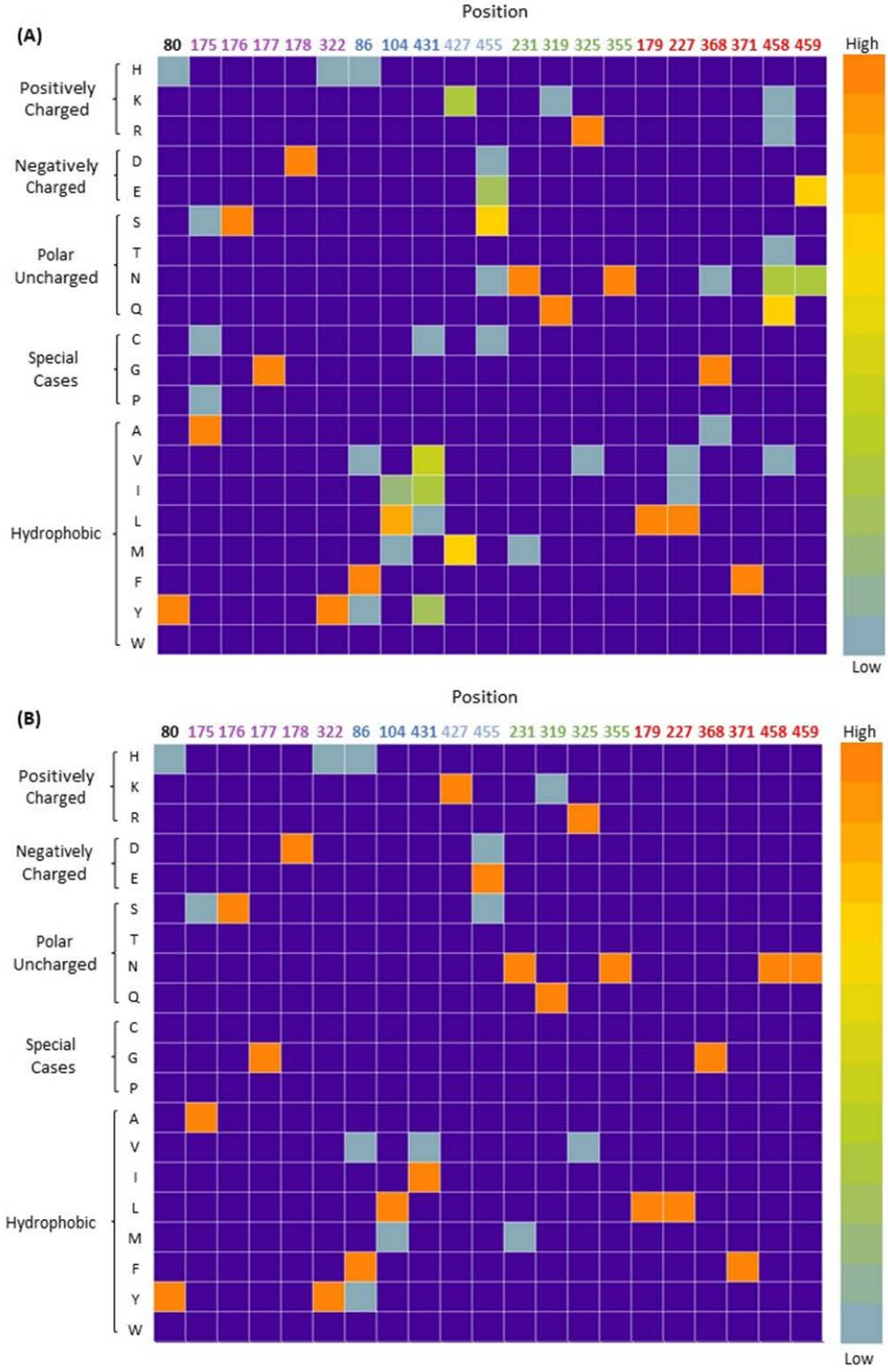

Figure 4. The results of the conservation analysis of the residues in the active site of TchPAM are revealed in a heatmap. The colors represent the appearance probability of the amino acids in the same position in homologues. The deep purple means that the residue has never mutated in this amino acid during the spontaneous mutation. The residues are colored according to their function (Figure 3). The conservation analysis was carried out by the multiple sequence alignment of homologues, including (**A**) all MIO-dependent enzymes or (**B**) PAM and PAL.

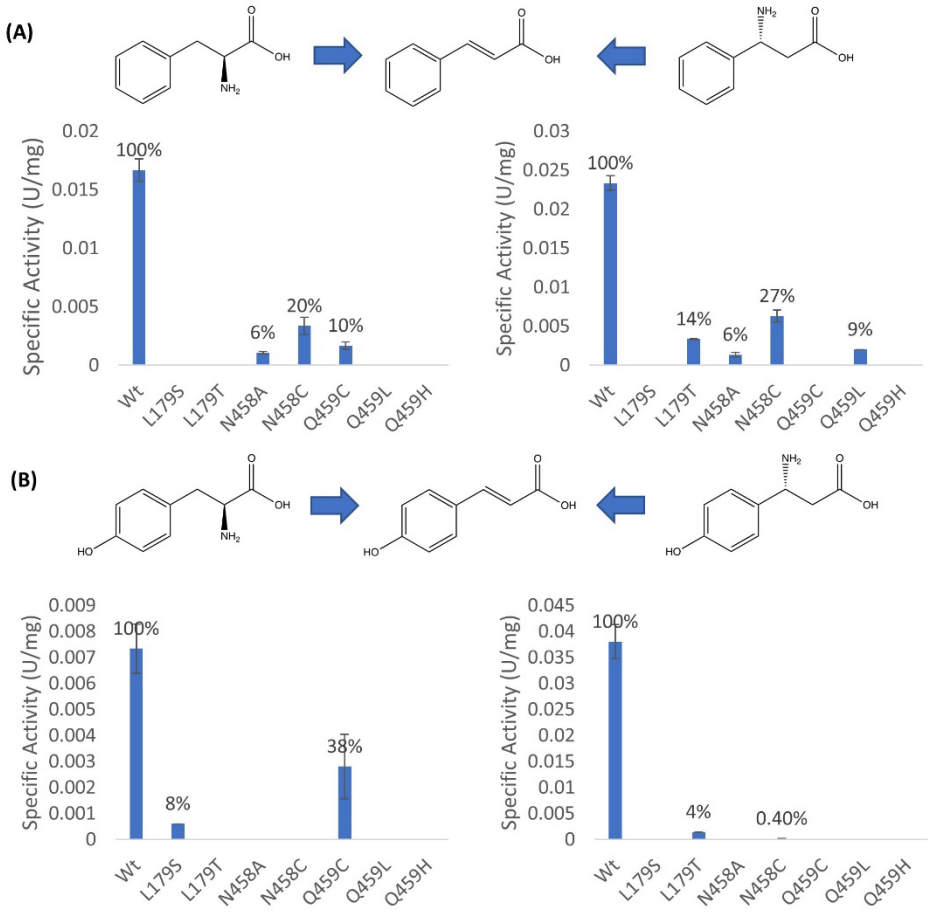

Figure 5. Comparison of specific activity in the ammonia elimination reaction of the designed mutants and the wild type of TchPAM with (**A**) (*S*)-α-phenylalanine, (*R*)-β-phenylalanine and (**B**) (*S*)-α-tyrosine, and (*R*)-β-tyrosine as the starting substrates. wt: wild type.

The residues Glu414 and Tyr280 (Gln459 and Tyr322 in TchPAM) have been described as electron acceptors to assist the two-step dehydration of the MIO loop in the previous molecular dynamics simulation study on PpHAL [13]. A similar conclusion was drawn by the structural investigation on TchPAM, highlighting the absence of the MIO prosthetic group in the mutant Tyr322Ala [21]. In contrast to the highly conserved residue Tyr322, the residue Gln459 can be naturally conservatively replaced by glutamic acid in the other member of the MIO-dependent enzyme family, indicating that it is not strictly required for MIO moiety formation.

In TchPAM, the partial positively charged formamide group of the residue Gln459 orients towards the edge of the aromatic ring of the substrate, driving the substrate away from the residue Gln459 [24] (Figure 6A), whereas the acidic residue in the other homologous at this position could push the aryl ring in the other direction due to the negatively charged ring center (Figure 6B). Upon the earlier mutagenesis study on TchPAM, the variant Arg325Lys/Gln459Glu was reported to improve the β-selectivity with lower activity, compared to the wild type [20]. Instead of the glutamine, the leucine with a hydrophobic side chain had a slightly attractive interaction with the aryl ring of the substrate in the mutant Gln459Leu, leading to the complete loss of activity with (*S*)-α-phenylalanine (Figure 6C). However, this mutant still accepted the (*R*)-β-phenylalanine as a substrate. Similarly, the Gln459Cys retained 10% activity to (*R*)-β-phenylalanine but could not catalyze the (*S*)-α-phenylalanine, which was caused by the lack of interaction between the side chain at this position and the aromatic ring of the substrate (Figure 6D). Compared to phenylalanine, the electron-rich tyrosine could increase the π-electron density, resulting in a larger diversion of the aryl ring of the substrate and the lack of activity in the mutant Gln459Leu [24,25].

While the mutant Gln459Cys retained partial activity with (*S*)-α-tyrosine, this could also indicate that the thiol group had less influence on the aryl ring due to the electronegativity. Moreover, the mutant Gln459His was not found to exhibit any lyase activity, which possibly suggests that the connection between the substrate and MIO moiety was hindered by the large side chain of histidine at this position. On the other hand, the steric constraint affected the formation of the MIO prosthetic group (Figure 6E). In summary, the residue Gln459 could affect the position of the aromatic group on the substrate. On the other hand, these results also proved the minimal difference in the binding position between (*S*)-α-, (*R*)-β-phenylalanine, and tyrosine, highlighting the importance of the residue Gln459 for the substrate selectivity.

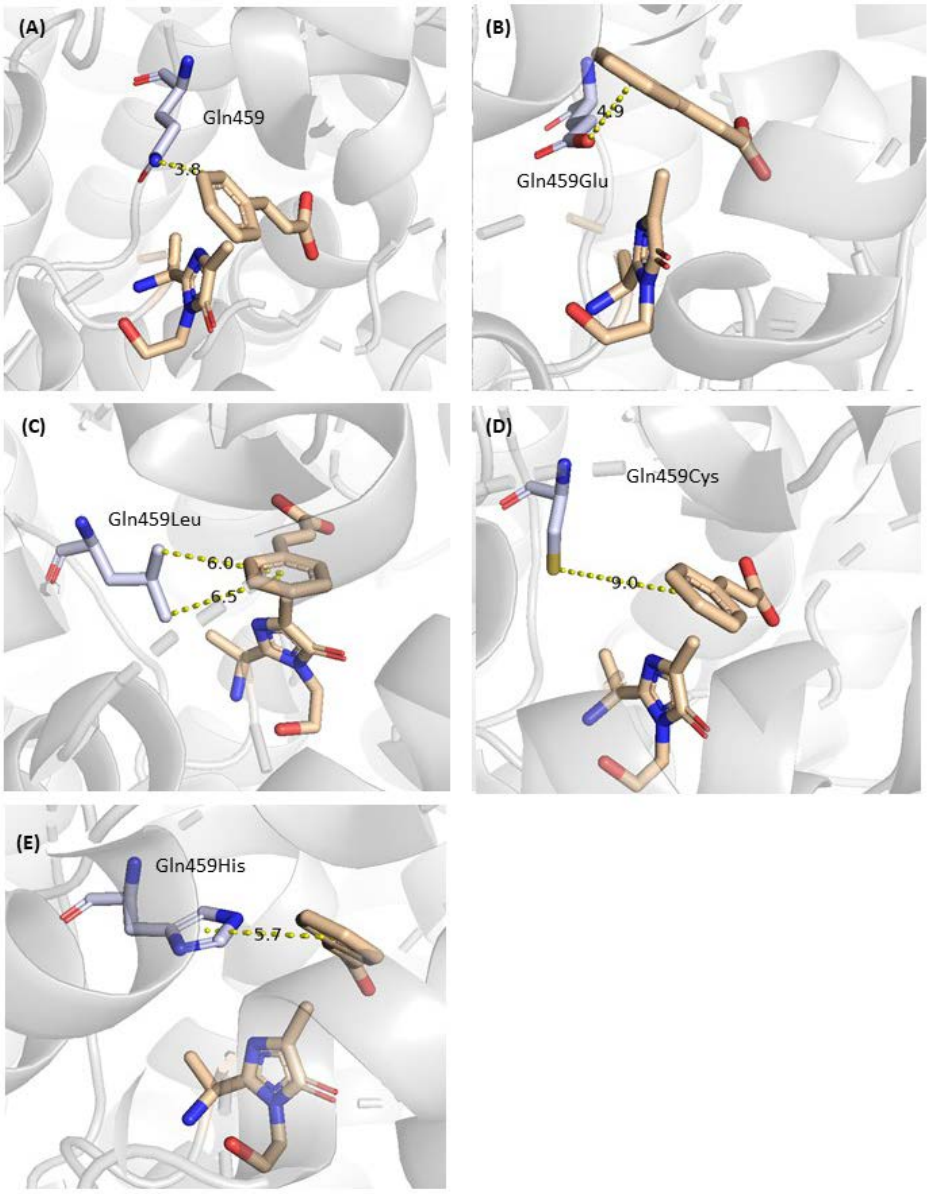

Figure 6. A key position for the positioning of the amino group from substrates: Gln459. The distance between the residue Gln459 and the aryl ring of the substrate in the wild type (**A**), the mutants Gln459Glu (**B**), Gln459Leu (**C**), Gln459Cys (**D**), and Gln459His (**E**).

The crystal structure of TchPAM bound to cinnamic acid showed that the residue Asn458 was located in the carboxyl binding pocket, which was not only near the residues Arg325 and Gln319 but was also in close contact with the substrate (Figure 7A). Even though the residue Asn458 mutated to Gln (68.0%), Arg, Thr, Lys, and Val in other MIO-

dependent enzymes, the formamide group seems to be preferred at this position in nature (>95%) (Figure 4). This formamide group could form a salt bridge to the carboxylate on the substrate during the binding of (*S*)-α-phenylalanine. Meanwhile, the neighboring residue Arg325 (approximately 4.4 Å), generally known as the key position for the binding of both α- and β-regioisomers, might be affected by the residue Asn458 due to steric and electronic considerations [26]. This inference was supported by the mutant Asn458Cys with decreased activity toward phenylalanine, especially the (*S*)-α-regioisomer. From the structural point of view, even though the carboxylate on the substrate could form a hydrogen bond with the thiol side chain, the interaction was absent in the mutant Asn458Cys due to the large distance (Figure 7B). Moreover, the interaction between the amino group from the residue Arg325 and the thiol group from the residue Asn458Cys was weaker than in the wild-type enzyme. Furthermore, the significant loss of activity in the mutant Asn458Ala with the breaking of the salt bridge suggests that the lack of steric hindrance caused by varying lengths of the side chain at this position might change the positioning of the neighboring residue (Figure 7C). In particular, this shift of residue Arg325 might change the binding mode of the β-phenylalanine and β-tyrosine, possibly reducing the attraction forces from the residues in the carboxyl binding pocket. In contrast to the wild type, the location of the bound substrates might be closer to the aromatic binding pocket in the mutants Asn458Ala and Asn458Cys without the salt bridge. Therefore, these mutants could not accept tyrosine as a substrate, which required more space in the aromatic binding pocket because of the phenolic ring. On the other hand, compared to the absence of the interaction between the residue Asn458 and the substrate, the shift of residue Arg325 seemed to be responsible for the reduction in the catalytic activity since the previous mutagenesis study revealed that the mutants Asn458Leu and Asn458Phe retained the identical activity as the wild type [27]. Moreover, replacing the residue Asn458 with alanine and cysteine might also influence the position of its neighboring residue Gln459, which could react with the amino group on the substrate.

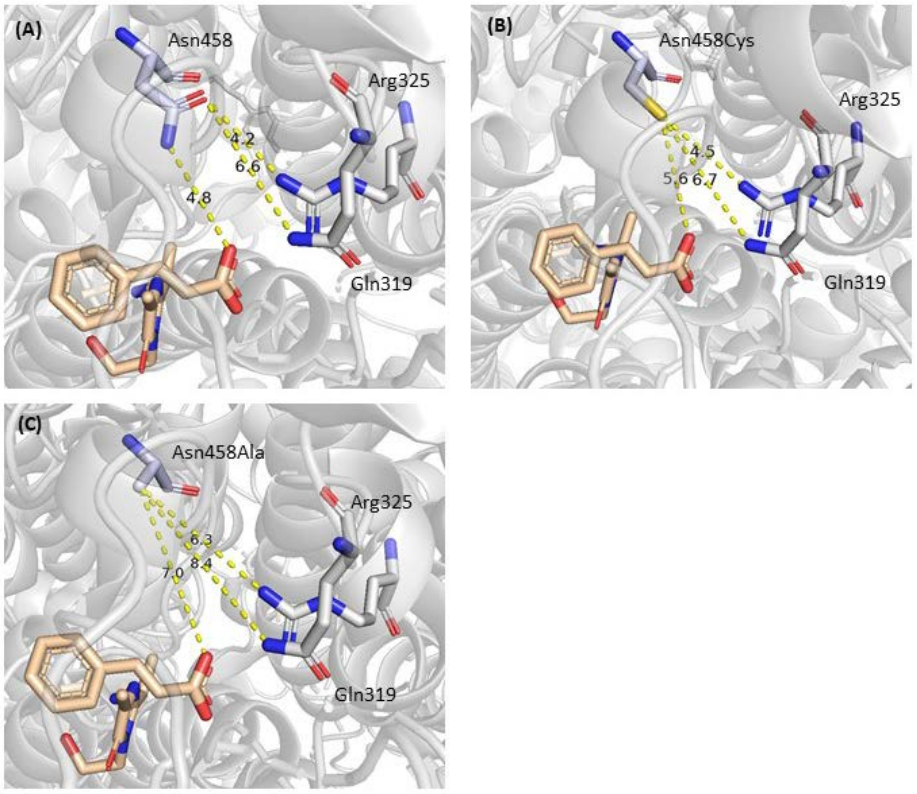

Figure 7. The carboxylate binding residue Asn458. The distance and proposed interaction between the residue Asn458 and the carboxylate group of the substrate, as well as the residues Gln319 and Arg325, shown in (**A**) wild type, (**B**) Asn458Cys, and (**C**) Asn458Ala.

2.2. Mutagenesis and Kinetic Analyses of the Residues Surrounding the Aryl Ring on Substrates

Earlier works have attempted to improve the β-regioselectivity of MIO-dependent enzymes through a variation of the residues in the aryl binding pocket, involving Phe86, Leu104, Cys107, Leu 108, and Leu179 [20,27]. During our previous mutagenesis studies, a binding pocket containing the residues Tyr424, Lys427, Ile431, and Glu455, was proposed to orient the substrate with phenolic acid and then to affect the regioselectivity and enantioselectivity of TchPAM [22]. To determine the potential influence of the substrate positioning on regioselectivity, the hydrophobic residues (Leu104, Leu108, and Ile431) from these binding pockets were selected and mutated. The kinetic parameters in the ammonia elimination reactions by the resulting enzyme variants were calculated by using (*S*)-α-phenylalanine, (*R*)-β-phenylalanine, (*S*)-α-tyrosine, and (*R*)-β-tyrosine as substrates (Table 1).

Table 1. Comparison of the kinetic parameters of wild type and mutants Leu104Ser, Leu108Ser, and Ile431Val in the ammonia elimination of various substrates.

		(*S*)-α-Phenylalanine	
TchPAM	**K_M (mM)**	**k_{cat} (s^{-1})**	**k_{cat}/K_M (mM^{-1} s^{-1})**
wt	0.032 ± 0.001	0.02 ± 0.001	0.625 ± 0.02
L104S	0.856 ± 0.019	0.133 ± 0.001	0.156 ± 0.003
L108S	0.02 ± 0.003	0.006 [a]	0.278 ± 0.004
I431V	0.028 ± 0.001	0.019 [a]	0.681 ± 0.026
		(*R*)-β-Phenylalanine	
TchPAM	**K_M (mM)**	**k_{cat} (s^{-1})**	**k_{cat}/K_M (mM^{-1} s^{-1})**
wt	0.062 ± 0.012	0.026 ± 0.002	0.427 ± 0.078
L104S	1.311 ± 0.308	0.098 ± 0.019	0.077 ± 0.019
L108S	0.039 ± 0.003	0.013 [a]	0.337 ± 0.035
I431V	0.076 ± 0.013	0.027 [a]	0.357 ± 0.059
		(*S*)-α-Tyrosine	
TchPAM	**K_M (mM)**	**k_{cat} (s^{-1})**	**k_{cat}/K_M (mM^{-1} s^{-1})**
wt	2.435 ± 0.160	0.029 ± 0.005	0.011 ± 0.002
L104S	-	-	-
L108S	-	-	-
I431V	0.506 ± 0.063	0.013 [a]	0.026 ± 0.002
		(*R*)-β-Tyrosine	
TchPAM	**K_M (mM)**	**k_{cat} (s^{-1})**	**k_{cat}/K_M (mM^{-1} s^{-1})**
wt	0.465 ± 0.008	0.06 ± 0.001	0.130 ± 0.01
L104S	2.715 ± 0.014	0.08 ± 0.016	0.030 ± 0.006
L108S	0.472 ± 0.054	0.021 ± 0.002	0.045 ± 0.001
I431V	0.618 ± 0.031	0.084 ± 0.003	0.137 ± 0.003

[a] The deviation is smaller as 0.001. wt: wild type. -: no activity.

According to the earlier structural studies on TchPAM, the closest distance between the *meta*-position of the aromatic ring from the substrate and the residue Leu104 was only 3.3 Å, which could provide a hydrophobic interaction during the binding of the substrate in the active site [17,21]. Moreover, this residue was confirmed as a steric constraining residue during the removal of ammonia for α-phenylalanine by the previous mutagenesis studies on TchPAM since the variant Leu104Ala displayed an increased catalytic efficiency and a decreased K_M value with 3- and 4-methyl-α-phenylalanine [17]. This consideration was also supported by similar engineering research on PcPAL from *Petroselinum crispum*,

the other family member of the MIO-dependent enzyme, revealing the favorable binding conformation of *o*- or *m*-methoxy α-phenylalanine in the active site of Leu134Ala (Leu104 in TchPAM) [28]. The kinetic studies showed that the mutant Leu104Ser displayed a reduction in catalytic efficiency with α- and β-phenylalanine due to the low binding affinities, which decreased by 26-fold and 21-fold compared to that of the wild type, respectively, indicating that this hydrophobic residue was essential for substrate binding. In addition, the mutation of the residue Leu104 to serine resulted in remarkably increased turnover numbers to α- and β-phenylalanine (around 6.5 and 3.7-fold improvement). This observation, combined with mutant Leu104Ala, giving a 6-fold increase in the turnover number to α-phenylalanine, suggested that either the hydrophobicity or length of this residue influenced the intermediate turnover [17]. Regarding tyrosine, the phenolic ring was sensitive to this variation by employing a polar residue in the aromatic binding pocket. The formation of a hydrogen bond interaction might have led to a deviation of the substrate orientation in the case with α-tyrosine, which was proved by the complete loss of the activity by replacing the residue Leu104 with serine. Despite the reduction in the binding affinity for all of the substrates in mutant Leu104Ser, this interaction seemed to have less influence on the deamination of β-tyrosine compared to the natural substrate.

The residue Leu108, which was recognized as the important position for switching the acceptance of different aromatic amino acids, could also affect the orientation of the aryl ring from the substrate due to its great hydrophobicity. The variation of residue leucine to a polar residue with one methylene shorter side chain could enhance the binding affinity for phenylalanine, in both α- and β-isoforms. Compared to the wild type, the mutant Leu108Ser displayed a 2.3-fold decreased catalytic efficiency with the natural substrate, α-phenylalanine, due to its considerably reduced turnover number, whereas the catalytic efficiency of β-phenylalanine was similar in the wild type and the mutant Leu108Ser. These results suggest that the hydrophobic residue Leu108 might not have such a huge influence on substrate binding, which could be explained by its far location from the bound substrate (>5 Å), in comparison with the other residues in the binding pockets. For a similar reason to the ammonia addition of α-tyrosine in mutant Leu104Ser, no activity was detected with the Leu108Ser mutant. However, this variant remained active to remove ammonia from β-tyrosine, albeit with a lower catalytic efficiency. Interestingly, this mutation did not change the binding affinity of the enzyme for β-tyrosine, suggesting that the phenolic ring on the substrate was likely oriented toward the other residues, unlike the case with α-tyrosine, which mitigated the influence of the hydrogen bond on the substrate positioning.

The residue Ile431 might be placed in the opposite position to residue Leu104, which could also provide a hindrance to the meta-substituted substrates [28]. According to the results from our previous mutagenesis study, the hydrophobic interaction between residue Ile431 and the aromatic amino acids was predominant and essential for the enzymatic catalysis since variants harboring mutations to Asn and Gln abolished the activity by using either α/β-phenylalanine or α/β-tyrosine as the starting substrate [22]. Compared to the wild type, the K_M and k_{cat} values of the mutant Ile431Val were changed slightly in the ammonia elimination of α- and β-phenylalanine. However, the mutation of the Ile431 to a smaller valine enhanced the binding affinity 4.8-fold with α-tyrosine as a substrate in comparison with the wild type. It seemed that the mutant Ile431Val afforded additional space, which could promote the binding of the phenolic ring on α-tyrosine in the active site. In contrast with α-tyrosine, the catalytic efficiency of mutant Ile431Val to β-tyrosine was similar to that of the wild type, indicating that the weaker hydrophobic interaction between the residue Ile431 and the phenolic ring had more influence on the binding of the β-tyrosine than the α-regioisomer.

As briefly demonstrated, the aryl rings from amino acids were bound in the aromatic binding pocket by two hydrophobic residues (Leu104 and Ile431), while the residue Leu108 provided a weaker interaction because of its farther position, leading to a relative loose binding site to the substrate.

2.3. Investigations into the Enantioselectivity of the Ammonia Addition Reactions

Since the discovery and isolation of the paclitaxel from the bark of *Taxus* species, TchPAM has received enormous attention due to its strict enantioselectivity. However, the mechanism of the ammonia addition at the β-position in only one (*R*)-conformer in TchPAM remained unclear which hindered the further development of the enantiopure aromatic amino acids production on an industrial scale. A comparison of the hydrophobic residues surrounding the bound substrate in the active site from the (*R*)-selective TchPAM and the PaPAM from *Pantoea agglomerans* with opposite enantioselectivity revealed some crucial differences in these dominating residues, particularly in the length of the side chain and the location in the aromatic binding pocket (Figure 8). Unlike the encircled aromatic binding pocket in TchPAM, the hydrophobic residues in PaPAM mainly occupied the inferoanterior position, which made a relatively loose binding pocket for the stabilization of the aryl ring from the substrate (Figure 8A). Moreover, the partial residues in PaPAM with a smaller side chain, such as Val108, and Leu421 (Leu108 and Ile431 in TchPAM) led to a weaker interaction between the bound substrate and the residues from the aromatic binding pocket, which also indicated that the aryl ring from the substrate could be relatively loosely bound in the active site in PaPAM. As an (S)-select phenylalanine aminomutase, PaPAM could catalyze the shift of the amino group of proteinogenic (*S*)-α-phenylalanine to yield its (*S*)-β-regioisomer. This reaction involves a minimal perturbation of the backbone position during the binding of intermediate *trans*-cinnamic acid in the active site [18,29]. The catalytic mechanism of ammonia readdition on the opposite face to afford (*R*)-β-phenylalanine has been debated extensively regarding the type of intermolecular rotation [17–20]. It also assumed the existence of a rotation around C_1-C_α and C_{ipso}-C_β bonds to bring the proton at the β-position and the MIO–amine adduct close to each other, considering the steric and torsional constraint from the methyl substituent [18]. Upon the energy calculation of the transition state and intermediate, the rearrangement reaction probably occurs through an approximately 180° rotation around the C_1-C_α bond [19]. On the other hand, the reorientation of cinnamic acid intermediate with the rotation around the C_{ipso}-C_β bond in the carboxyl binding pocket could also promote the isomerization reaction, supported by the results from the site-directed mutagenesis of the residues Arg325 and Gln319 [20].

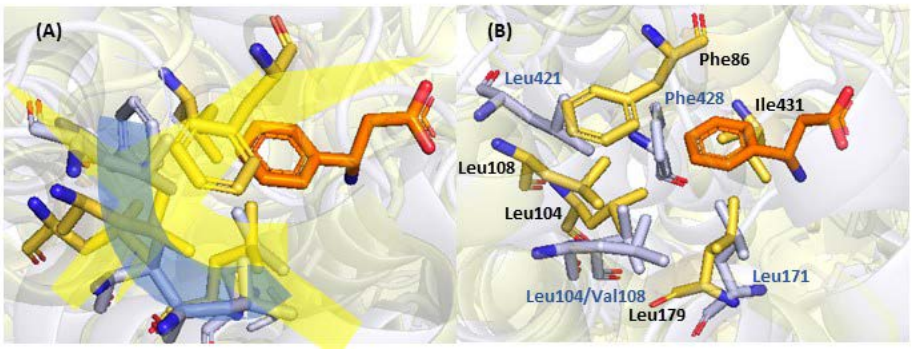

Figure 8. Overlay of the hydrophobic residues in the active site of (*R*)-selective TchPAM (yellow, PDB ID: 4C5R) and (*S*)-selective PaPAM (purple, PDB ID: 3UNV). The ligand is β-phenylalanine, which is colored in orange. (**A**) the top view shows the enclosed aromatic binding pocket in TchPAM (yellow line) and the semi-enclosed aromatic binding pocket in PaPAM (blue line). (**B**) the side view shows the involved hydrophobic residues (TchPAM: black, PaPAM: blue).

To investigate the (*R*)-selectivity of TchPAM in this work, the conversion rate and the enantiomeric excess of the mutants were confirmed through HPLC with OPA/IBLC derivatization. Interestingly, the mutant Leu104Ser could generate the (*S*)-β-phenylalanine, albeit with a conversion of only 7% after 24 h. However, the (*S*)-β-phenylalanine was not found as a product through the catalysis by the wild type and the mutant Ile431Val. By contrast, the variation of residue Ile431 to valine led to an enantioselectivity switch, yielding the (*S*)-β-tyrosine as the favorable product (ee_S > 29%) from *trans*-*p*-hydroxycinnamic acid.

The mutant Ile431Val had the specific activities of 0.23 ± 0.006 U/mg for the production of (*S*)-β-tyrosine and 0.04 ± 0.009 U/mg for the production of (*R*)-β-tyrosine, respectively.

The above-mentioned hypotheses, combined with the measurement of the conversion rate and enantiomeric excess in ammonia addition reaction by the wild type and mutants, allowed a proposed isomerization mechanism with additional details to establish. As shown in Figure 9, when (*S*)-α-phenylalanine entered the active site of TchPAM, it would bind owing to the bidentate salt bridge with the residue Arg325 on the carboxylate side, stabilized by the hydrophobic residues Phe86, Leu104, and Ile431 on the aromatic side. In TchPAM, the interaction between the aryl ring of the substrate and the hydrophobic residues is stronger than in the (*S*)-β-selective PaPAM, avoiding the shift in the backbone of the substrate and readdition of the ammonia on the respective (*S*)-β-position. To promote the reamination on the opposite face, the conformer interchange of *trans*-cinnamic acid intermediate could be carried by a bond rotation, leading to the rebinding of the carboxyl binding group with the residues Arg325, Asn231, and Asn355. Herein, the single rotation around the C_{ipso}-C_β bond would be preferred over the rotation around C_1-C_α bond with the flipping of the whole aryl ring on the substrate or both bonds together due to the steric and torsional considerations [20].

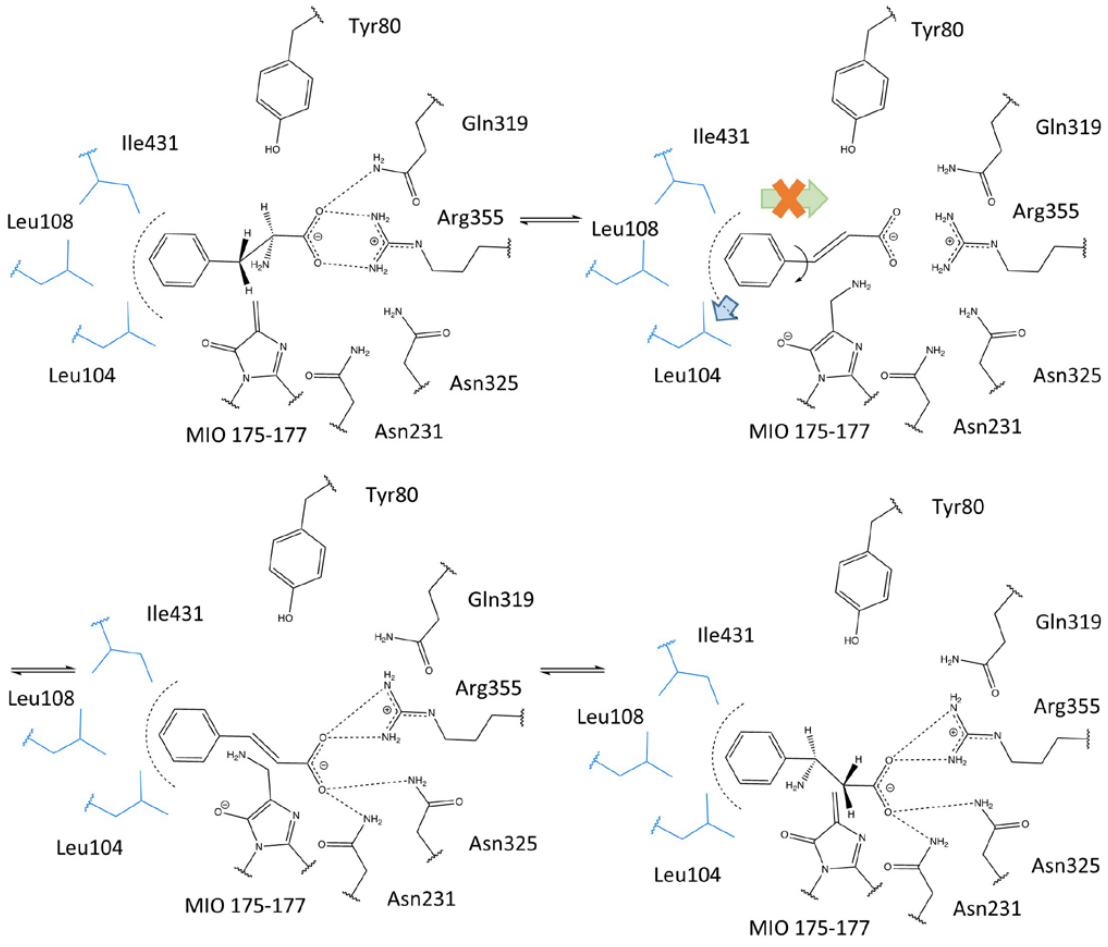

Figure 9. Proposed isomerization mechanism of (*R*)-selective TchPAM. When (*S*)-α-phenylalanine enters the active site of TchPAM, its carboxylate group is stabilized by residues Arg325 and Gln319. In the wild-type enzyme, the benzene ring is fixed in the aromatic binding pocket, in particular, with the residue Leu104, during the ammonia elimination to form the cinnamic intermediate. A single rotation around the C_{ipso}-C_β bond without breaking the interaction with residue Leu104 brings the β-position on α,β-unsaturated acid to a suitable position for the readdition reaction by the MIO–amine adduct, giving (*R*)-β-phenylalanine as the product. Meanwhile, the carboxylate group from the intermediate is stabilized by residues Arg325, Asn231, and Asn355.

The variation of the hydrophobic residue Leu104 to serine with a polar side chain reduced the interaction with the aryl ring from the substrate, mitigating the need for rotation and leading to a change of enantioselectivity of TchPAM (Figure 10). Further supporting evidence was derived from the structure of (*S*)-selective PaPAM with a relatively loose aromatic binding pocket. Because of the electron-rich aryl ring, the tyrosine is oriented towards the binding pocket with the residues Tyr424, Lys427, Ile431, and Glu455 during the binding of the substrate and intermediate in the active site of TchPAM [22]. Therefore, the weakening of the interaction between the aryl ring of the intermediate and the hydrophobic residue Ile431 led to a larger deviation, which was consistent with the enantioselectivity of TchPAM towards (*S*)-β-tyrosine, but not (*S*)-β-phenylalanine. From a similar catalytic point of view, the production of (*S*)-β-tyrosine could be attributed to the decreased London dispersion force by valine with a smaller hydrophobic side chain on position 431. Furthermore, no activity was detected with the mutant Leu108Ser by using *trans-p*-hydroxycinnamic acid as a substrate, suggesting that the interaction with this hydrophobic residue was weaker than the residue Ile431, which could be explained by its farther location (>5 Å) from the phenolic ring.

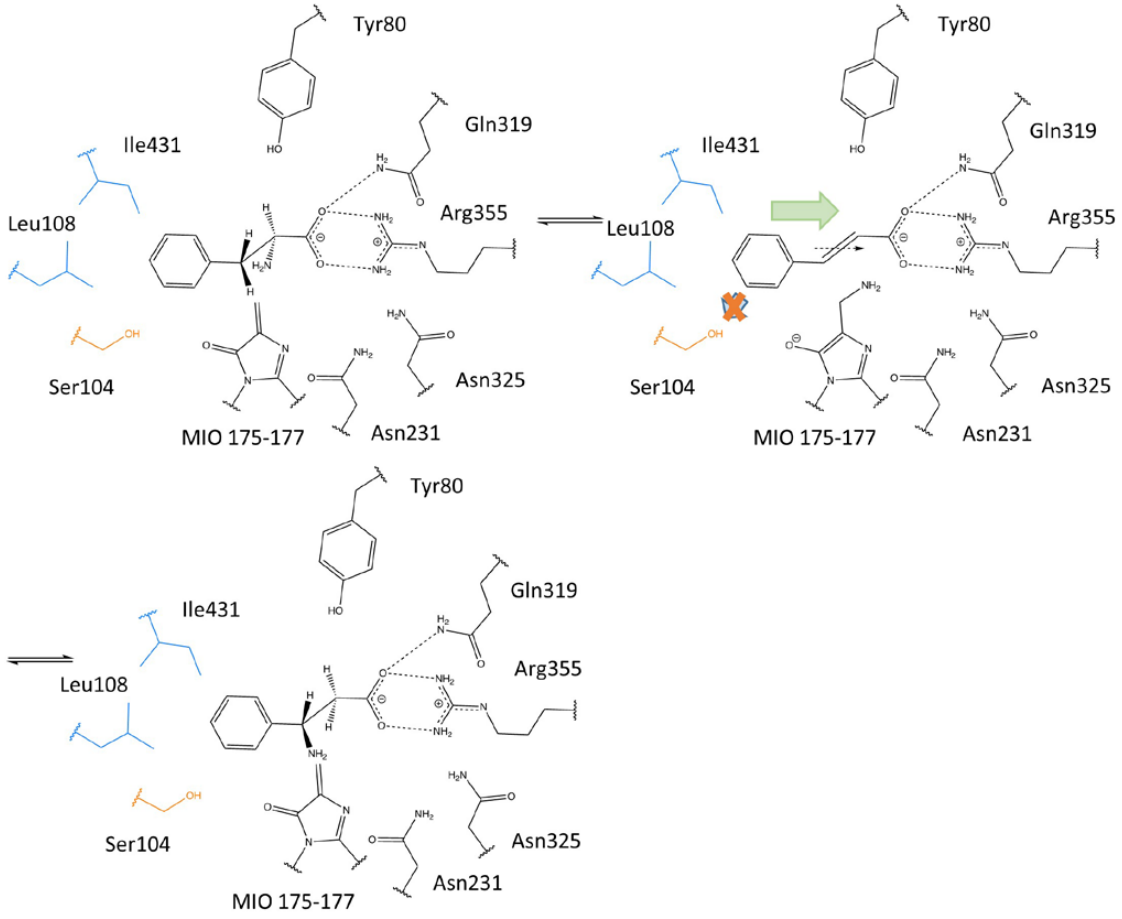

Figure 10. In the mutant Leu104Ser, the benzene ring can move in the aromatic binding pocket due to the lack of a hydrophobic residue at position 104 during the ammonia elimination to form the cinnamic acid intermediate. Thus, the minimal shift of the intermediate backbone led to an immediate readdition of ammonia on the β-position, as well as the formation of (*S*)-β-phenylalanine.

Considering the distribution of the enantioselectivity among the MIO-dependent enzymes, the torsional energy for the interconversion might be not the principal factor to prevent the rearrangement with any sort of bond rotation. It was reasoned that the vast majority of the phenylalanine- and tyrosine aminomutase produced both (*R*)- and (*S*)-β-amino acids in a distinct ratio. As such, the high enantioselectivity of TchPAM could

be ascribed to the steric strain between the surrounding residues and the aryl ring from the substrate. Among them, the residue Leu104 seemed to be crucial for the maintenance of the perfect enantioselectivity in TchPAM since it was the closest hydrophobic residue to the aromatic ring of the α-amino acids after substrate binding [17], whereas the mutant Ile431Val played a more important role in the enantiopreference of β-tyrosine.

3. Conclusions

TchPAM has received enormous attention due to its ability to catalyze the *trans*-cinnamic acid and produce enantiopure (*R*)-β-phenylalanine, which are considered as the chiral building blocks of bioactive products. In recent years, various research groups have explored the influence of the major residues in the active site of the enzyme through mutagenesis experiments, in silico studies, and structure analysis. However, the function of some residues, which were located in close contact with the binding position of substrates in 5 Å, remained enigmatic. In this work, the proposed function of these residues was investigated and discussed. Among them, the highly conserved residue Leu179 was confirmed to be necessary for activity by the stabilization of the aryl ring of the substrate, not the MIO moiety formation. The site-directed mutagenesis of TchPAM allowed the identification of the residue Gln459 as an essential position for substrate selectivity, since the interaction between the side chain of the residue Gln459 and the aryl ring of the substrate affected the binding position, leading to different substrate preferences. Its neighboring residue Asn458 affects the substrate positioning with the salt bridge between the carboxylate group of the substrate and may influence the residues in the carboxyl binding pocket of the enzyme. The function of the surrounding residues in the active site of TchPAM is summarized in Table 2. These results may act as a cornerstone for the rational engineering of MIO-dependent enzymes to increase the activity, expand the scope of the substrate, and improve the enantioselectivity in the future. Moreover, the reaction temperature could also be a key factor that influences the mutase activity of TchPAM by changing the inner loop structure [30]. It should be an attractive area in the future study on TchPAM.

Table 2. A summary of the dividing residue groups with the proposed functions.

Group Number	Containing the Residues	Function	Reference
1	Tyr80	Activation	[21,31]
2	Ala175, Ser176, Gly177, Asp178, Tyr322	MIO moiety Formation	[11,13,21]
3	Asn231, Gln319, Arg325, Asn458	Carboxylate Binding	[20], this work
4	Phe86, Leu104, Leu108, Leu179, Ile431	Aromatic group Binding	[20], this work
5	Cys107, Tyr424, Lys427, Glu455, Gln459	Influence on the neighboring Residues	[22], this work
6	Leu227, Gly368, Phe371	unknown	
7	Ala77, Ile79, Cys89, Leu97	Flexibility of inner loop, selectivity of mutase/lyase activity	[32]

The bond between the aryl ring from the substrate and the intermediate was more flexible in the active site of (*R*)-selective enzyme TchPAM. Therefore, variation of the hydrophobic residues in the aromatic binding site with smaller or polar side chains leads to an improved enantiopreference of (*S*)-β-aromatic amino acids as the product. From these findings, combined with the structural comparison with (*S*)-selective PaPAM, an isomerization mechanism was proposed for the explanation of the strict enantioselectivity of TchPAM. During the ammonia readdition reaction, the aryl ring from the intermediate *trans*-cinnamic acid and *trans-p*-hydroxycinnamic acid was fixed by the hydrophobic residues Leu104 and Ile431, respectively. The reorientation of carboxylate from the unsaturated intermediate

group could be attributed to the 180° rotation around the C_{ipso}-C_{β} bond, promoting the subsequent attachment of the MIO–amine adduct at the (*R*)-β-position. An investigation into the TchPAM with strict enantioselectivity could promote the establishment of the chemoenzymatic cascades involving the (*R*)-β-aromatic amino acids, raising the possibility for the development of large-scale productions of β-amino acids using aminomutases. Moreover, this study represents one of the most promising strategies to produce the β-amino acids in the biocatalysis industry, such as limiting waste for the synthesis of complex drug structures and enabling more straightforward synthesis routes [8].

4. Materials and Methods

4.1. Computational Enzyme Design and Conservation Analysis

The TchPAM was designed using PyRosetta [33]. The target substrate and MIO prosthetic group were created using the OpenBabel 2.4 software [34]. After the optimization of the transition state geometries of these small molecules in Gaussian09 [35], the conformers were generated through the Biology and Chemistry Library Project (BCL) [36]. The starting coordinates of the natural substrate in the active center of TchPAM (PDB ID: 4C5R) were confirmed according to the PDB file. To select the best mutants, the resulting designs were evaluated through a calculation of the catalytic constraints from PyRosetta and a structural analysis using the visualization system PyMOL [37].

The homologues of TchPAM with a sequence similarity of over 30% were identified from SwissProt and classified into two parts. The enzymes with phenylalanine aminomutase or ammonia-lyase activity were summarized in the first one. The other part contained all MIO-dependent enzymes (PAM, PAL, TAM, TAL, and HAL). The multiple sequence alignments were carried out by using MAFFT version 7.3 [38].

4.2. Construction of the TchPAM Mutants

Based on the protein sequence from *Taxus chinesis* (NCBI, AY724735.1), the codon-optimized *pam* gene, ligating into vector plasmid pET28a (+) with an N-terminal His-Tag, was synthesized commercially by ProteoGenix (France). To minimize off-target priming, a touch-down PCR was employed in a site-directed mutagenesis using Q5® High-Fidelity 2X Master Mix (NEB, Ipswich, MA, USA). The primers were supplied by Thermo Fisher Scientific (Waltham, MA, USA) (Table 3). Then, after digest by DpnI for 1 h, the PCR products were transformed into high efficiency chemically T7 express competent *E. coli* (NEB, Ipswich, USA). All mutations were confirmed by DNA sequencing services from GATC (Ebersberg, Germany).

Table 3. List of primers in site-directed mutagenesis.

Mutant	Direction	Primer-Sequence
L104S	fw	CTG CAG GAA AGT AGC ATT CGC TGT CT
	rw	ACT TTC CTG CAG TTC GCT CAG G
L108S	fw	CTG ATT CGC TGT AGC CTG GCA G
	rw	ACA GCG AAT CAG ACT TTC CTG CA
L179S	fw	GCA AGC GGC GAT AGC ATT CCG
	rw	ATC GCC GCT TGC GCT AAC A
L179T	fw	GCA AGC GGC GAT ACC ATT CCG
	rw	ATC GCC GCT TGC GCT AAC A
I431V	fw	AAA GGT CTG GAT GTT GCA ATG GCC
	rw	ATC CAG ACC TTT CAG GCC ATA ATC
N458A	fw	GCA GAA CAG CAT GCA CAG GAT ATT AAT A
	rw	ATG CTG TTC TGC ACT ATG CAC A
N458C	fw	GCA GAA CAG CAT TGC CAG GAT ATT AAT A
	rw	ATG CTG TTC TGC ACT ATG CAC A
Q459C	fw	AGA ACA GCA TAA TTG CGA TAT TAA TAG TCT G
	rw	ATT ATG CTG TTC TGC ACT ATG CAC
Q459L	fw	AGA ACA GCA TAA TCT GGA TAT TAA TAG T
	rw	ATT ATG CTG TTC TGC ACT ATG CAC
Q459H	fw	AGA ACA GCA TAA TCA CGA TAT TAA TAG T
	rw	ATT ATG CTG TTC TGC ACT ATG CAC

4.3. Expression, Purification, and Concentration of TchPAM

The cells were grown at 37 °C with 120 rpm shaking in an LB-medium, containing 50 μg/mL kanamycin. Until OD_{600} reached 0.3–0.4, the culture was continually shaken for another 22 h at 25 °C after adding 0.1 mM isopropyl β-d-thiogalactopyranoside for induction. The collected cells were washed with 50 mM Tris HCl buffer (pH 8) twice and resuspended in a binding buffer (containing 50 mM Tris-HCl, 150 mM NaCl, and 10 mM imidazole, pH 8) for sonication (20 s pulse/30 s pause, 40% amplitude, HD3100, Bandelin electronic GmbH & Co. KG, Berlin, Germany). The crude enzymes were obtained by centrifugation for 20 min at 16,000 g and 4 °C (Thermo Fisher Scientific Inc., Waltham, Massachusetts, USA), which were purified by His SpinTrap column (GE Healthcare, Chicago, IL, USA), according to the protocol from the company. To remove the imidazole and concentrate the pure enzyme, the protein concentrators (10 K MWCO, Pierce® Concentrator, Thermo Fisher Scientific, Waltham, MA, USA) were applied. The pure enzymes, whose purity was controlled through SDS-PAGE electrophoresis, were diluted in 0.5 mg/mL and prepared for enzyme characterization.

4.4. Kinetic Analysis of the Ammonia Elimination Reaction

In order to determine the kinetic parameters of the wild type and mutants of TchPAM with various aromatic amino acids: (*S*)-α-, (*R*)-β-phenylalanine and (*S*)-α-, (*R*)-β-tyrosine, 10 mM substrate stock was prepared in 50 mM Tris-HCl buffer, pH 8.8, except for (*S*)-α-phenylalanine with a maximal concentration in 2 mM, which had poor solubility in the reaction buffer. The measurement was carried out in preheated 96 well UV-Microplates (Greiner Bio-One, Monroe, NC, USA). Each well contained 100 μL of substrate solution, which was diluted with the following concentrations: 0, 0.01, 0.05, 0.1, 0.2, 0.5, 1, 2, 5 and 10 mM. After pipetting 10 μL of pure enzymes, the reaction was performed at 40 °C and 600 rpm. The absorbance was measured for 20 min with intervals of 2 min to determine the concentration of the produced corresponding unsaturated acid, at 290 and 350 nm for cinnamic acid and hydroxycinnamic acid, respectively. Kinetic parameters (K_M, V_{max}) were calculated by Origin (Pro 2019, OriginLab®, Northampton, MA, USA).

4.5. HPLC Analysis of the Ammonia Addition Reaction

A total of 50 μL of the purified enzyme was added to 500 μL of preheated ammonium sulfate solution (4M, pH 10), containing 3 mM *trans-p-* hydroxycinnamic acid as substrate. After different time intervals, 50 μL of samples were taken from the reaction mixture, which was incubated at 40 °C, quenched by heating for 5 min at 99 °C, vortexed, and centrifuged. For the determination of the enantiomeric excess values, the supernatant was derivatized in a precolumn using *o*-phthalaldehyde (OPA) with isobuteryl-l-cysteine (IBLC) before injection into the HPLC column (C18, 150 × 4.6 mm HyperClone 5 μm, Phenomenex Inc, Torrance, CA, USA) [39,40]. The derivatization reagent containing the mixture of methanolic OPA solution and IBLC solution (in 0.1 M borate buffer) in molar ratio 1:3, was always freshly prepared. Elution was performed with different gradients of the mobile phase of 40 mM sodium phosphate buffer (pH 6.5) (eluent A, 21%) and methanol (eluent B, 79%) and a constant flow rate of 1.0 mL/min. The formation of aromatic amino acids was detected at 380 nm with different retention times: (*S*)-α-tyrosine 71.0 min, (*R*)-α-tyrosine 45.7 min, (*S*)-β-tyrosine 57.6 min, (*R*)-β-tyrosine 42.7 min.

Author Contributions: Conceptualization and supervision, J.R.; methodology, U.E. and F.P.; high-performance computer, H.A.; computational enzyme design, conserved residues analysis, characterization of the designed enzymes through UV spectroscopy and HPLC, writing the manuscript, F.P.; revising the manuscript, J.R., U.E., A.D. and H.A. All authors have read and agreed to the published version of the manuscript.

Funding: This work is supported by the China Scholarship Council and is part of the bioeconomy graduate program BBW ForWerts of the German state of Baden-Württemberg. We gratefully thank the Open Access Publishing Fund of Karlsruhe Institute of Technology.

Conflicts of Interest: The authors declare no conflict of interest.

References

1. Juaristi, E.; Soloshonok, V.A. *Enantioselective Synthesis of Beta-Amino Acids*; John Wiley & Sons: London, UK, 2005.
2. Cabrele, C.; Martinek, T.A.; Reiser, O.; Berlicki, Ł. Peptides containing β-amino acid patterns: Challenges and successes in medicinal chemistry. *J. Med. Chem.* **2014**, *57*, 9718–9739. [CrossRef] [PubMed]
3. Xue, Y.-P.; Cao, C.-H.; Zheng, Y.-G. Enzymatic asymmetric synthesis of chiral amino acids. *Chem. Soc. Rev.* **2018**, *47*, 1516–1561. [CrossRef] [PubMed]
4. Slichenmyer, W.J.; Von Hoff, D.D. Taxol: A new and effective anti-cancer drug. *Anticancer Drugs* **1991**, *2*, 519–530. [CrossRef] [PubMed]
5. Malik, S.; Cusidó, R.M.; Mirjalili, M.H.; Moyano, E.; Palazón, J.; Bonfill, M. Production of the anticancer drug taxol in Taxus baccata suspension cultures: A review. *Process Biochem.* **2011**, *46*, 23–34. [CrossRef]
6. Weaver, B.A. How Taxol/paclitaxel kills cancer cells. *Mol. Biol. Cell* **2014**, *25*, 2677–2681. [CrossRef]
7. Thornburg, C.K.; Walter, T.; Walker, K.D. Biocatalysis of a paclitaxel analogue: Conversion of baccatin III to N-debenzoyl-N-(2-furoyl) paclitaxel and characterization of an amino phenylpropanoyl CoA transferase. *Biochemistry* **2017**, *56*, 5920–5930. [CrossRef]
8. Zhang, G.; Liang, Y.; Qin, T.; Xiong, T.; Liu, S.; Guan, W.; Zhang, Q. Copper-Catalyzed Asymmetric Hydroamination: A Unified Strategy for the Synthesis of Chiral $β$-Amino Acid and Its Derivatives. *CCS Chem.* **2021**, *3*, 1737–1745. [CrossRef]
9. Turner, N.J. Ammonia lyases and aminomutases as biocatalysts for the synthesis of α-amino and β-amino acids. *Curr. Opin. Chem. Biol.* **2011**, *15*, 234–240. [CrossRef]
10. Schwede, T.F.; Rétey, J.; Schulz, G.E. Crystal structure of histidine ammonia-lyase revealing a novel polypeptide modification as the catalytic electrophile. *Biochemistry* **1999**, *38*, 5355–5361. [CrossRef]
11. Baedeker, M.; Schulz, G.E. Autocatalytic peptide cyclization during chain folding of histidine ammonia-lyase. *Structure* **2002**, *10*, 61–67. [CrossRef]
12. Reid, B.G.; Flynn, G.C. Chromophore formation in green fluorescent protein. *Biochemistry* **1997**, *36*, 6786–6791. [CrossRef] [PubMed]
13. Sánchez-Murcia, P.A.; Bueren-Calabuig, J.A.; Camacho-Artacho, M.; Cortés-Cabrera, Á.; Gago, F. Stepwise Simulation of 3,5-Dihydro-5-methylidene-4H-imidazol-4-one (MIO) Biogenesis in Histidine Ammonia-lyase. *Biochemistry* **2016**, *55*, 5854–5864. [CrossRef] [PubMed]
14. Punekar, N.S. *Enzymes: Catalysis, Kinetics and Mechanisms*; Springer: Berlin/Heidelberg, Germany, 2018.
15. Chesters, C.; Wilding, M.; Goodall, M.; Micklefield, J. Thermal bifunctionality of bacterial phenylalanine aminomutase and ammonia lyase enzymes. *Angew. Chem. Int. Ed.* **2012**, *51*, 4344–4348. [CrossRef] [PubMed]
16. Bartsch, S.; Wybenga, G.G.; Jansen, M.; Heberling, M.M.; Wu, B.; Dijkstra, B.W.; Janssen, D.B. Redesign of a phenylalanine aminomutase into a phenylalanine ammonia lyase. *ChemCatChem* **2013**, *5*, 1797–1802. [CrossRef]
17. Feng, L.; Wanninayake, U.; Strom, S.; Geiger, J.; Walker, K.D. Mechanistic, mutational, and structural evaluation of a taxus phenylalanine aminomutase. *Biochemistry* **2011**, *50*, 2919–2930. [CrossRef]
18. Ratnayake, N.D.; Wanninayake, U.; Geiger, J.H.; Walker, K.D. Stereochemistry and mechanism of a microbial phenylalanine aminomutase. *J. Am. Chem. Soc.* **2011**, *133*, 8531–8533. [CrossRef]
19. Wang, K.; Hou, Q.; Liu, Y. Insight into the mechanism of aminomutase reaction: A case study of phenylalanine aminomutase by computational approach. *J. Mol. Graph. Model.* **2013**, *46*, 65–73. [CrossRef]
20. Wu, B.; Szymański, W.; Wybenga, G.G.; Heberling, M.M.; Bartsch, S.; Dewildeman, S.; Poelarends, G.J.; Feringa, B.L.; Dijkstra, B.W.; Janssen, D.B. Mechanism-inspired engineering of phenylalanine aminomutase for enhanced β-regioselective asymmetric amination of cinnamates. *Angew. Chem. Int. Ed.* **2012**, *51*, 482–486. [CrossRef]
21. Wybenga, G.G.; Szymanski, W.; Wu, B.; Feringa, B.L.; Janssen, D.B.; Dijkstra, B.W. Structural investigations into the stereochemistry and activity of a phenylalanine-2,3-aminomutase from Taxus chinensis. *Biochemistry* **2014**, *53*, 3187–3198. [CrossRef]
22. Peng, F.; Aliyu, H.; Delavault, A.; Engel, U.; Rudat, J. Computational-Designed Enzyme for β-Tyrosine Production in Lignin Valorization. *Catalysts* **2021**, *11*, 1310. [CrossRef]
23. Ribeiro, A.J.M.; Tyzack, J.D.; Borkakoti, N.; Holliday, G.L.; Thornton, J.M. A global analysis of function and conservation of catalytic residues in enzymes. *J. Biol. Chem.* **2020**, *295*, 314–324. [CrossRef] [PubMed]
24. Janiak, C. A critical account on π-π stacking in metal complexes with aromatic nitrogen-containing ligands. *J. Chem. Soc. Dalt. Trans.* **2000**, 3885–3896. [CrossRef]
25. McGaughey, G.B.; Gagné, M.; Rappé, A.K. π-Stacking interactions. Alive and well in proteins. *J. Biol. Chem.* **1998**, *273*, 15458–15463. [CrossRef] [PubMed]

26. Wu, B.; Szymanski, W.; Wietzes, P.; de Wildeman, S.; Poelarends, G.J.; Feringa, B.L.; Janssen, D.B. Enzymatic synthesis of enantiopure α- and β-amino acids by phenylalanine aminomutase-catalysed amination of cinnamic acid derivatives. *ChemBioChem* **2009**, *10*, 338–344. [CrossRef]
27. Zhu, L.; Ge, F.; Li, W.; Song, P.; Tang, H.; Tao, Y.; Liu, Y.; Du, G. One step synthesis of unnatural β-arylalanines using mutant phenylalanine aminomutase from *Taxus chinensis* with high β-regioselectivity. *Enzym. Microb. Technol.* **2018**, *114*, 22–28. [CrossRef]
28. Nagy, E.Z.A.; Tork, S.D.; Lang, P.A.; Filip, A.; Irimie, F.D.; Poppe, L.; Toşa, M.I.; Schofield, C.J.; Brem, J.; Paizs, C.; et al. Mapping the Hydrophobic Substrate Binding Site of Phenylalanine Ammonia-Lyase from Petroselinum crispum. *ACS Catal.* **2019**, *9*, 8825–8834. [CrossRef]
29. Strom, S.; Wanninayake, U.; Ratnayake, N.D.; Walker, K.D.; Geiger, J.H. Insights into the mechanistic pathway of the Pantoea agglomerans phenylalanine aminomutase. *Angew. Chem. Int. Ed.* **2012**, *51*, 2898–2902. [CrossRef]
30. Pilbák, S.; Tomin, A.; Rétey, J.; Poppe, L. The essential tyrosine-containing loop conformation and the role of the C-terminal multi-helix region in eukaryotic phenylalanine ammonia-lyases. *FEBS J.* **2006**, *273*, 1004–1019. [CrossRef]
31. Röther, D.; Poppe, L.; Morlock, G.; Viergutz, S.; Rétey, J. An active site homology model of phenylalanine ammonia-lyase from *Petroselinum crispum*. *Eur. J. Biochem.* **2002**, *269*, 3065–3075. [CrossRef]
32. Heberling, M.M.; Masman, M.F.; Bartsch, S.; Wybenga, G.G.; Dijkstra, B.W.; Marrink, S.J.; Janssen, D.B. Ironing out their differences: Dissecting the structural determinants of a phenylalanine aminomutase and ammonia lyase. *ACS Chem. Biol.* **2015**, *10*, 989–997. [CrossRef]
33. Chaudhury, S.; Lyskov, S.; Gray, J.J. PyRosetta: A script-based interface for implementing molecular modeling algorithms using Rosetta. *Bioinformatics* **2010**, *26*, 689–691. [CrossRef] [PubMed]
34. Boyle, N.M.O.; Banck, M.; James, C.A.; Morley, C.; Vandermeersch, T.; Hutchison, G.R. Open Babel: An open chemical toolbox. *J. Cheminform.* **2011**, *3*, 33. [CrossRef] [PubMed]
35. Frisch, M.J.; Trucks, G.W.; Schlegel, H.B.; Scuseria, G.E.; Robb, M.A.; Cheeseman, J.R.; Scalmani, G.; Barone, V.; Petersson, G.A.; Nakatsuji, H.; et al. *Gaussian 09*; Revision A.02; Gaussian Inc.: Oxford, UK, 2016.
36. Kothiwale, S.; Mendenhall, J.L.; Meiler, J. BCL::Conf: Small molecule conformational sampling using a knowledge based rotamer library. *J. Cheminform.* **2015**, *7*, 47. [CrossRef] [PubMed]
37. Schrödinger, LLC. *The {PyMOL} Molecular Graphics System*; Version 1.8; Schrodinger Inc.: New York, NY, USA, 2015.
38. Katoh, K.; Standley, D.M. MAFFT multiple sequence alignment software version 7: Improvements in performance and usability. *Mol. Biol. Evol.* **2013**, *30*, 772–780. [CrossRef]
39. Brückner, H.; Wittner, R.; Godel, H. Automated enantioseparation of amino acids by derivatization with o-phthaldialdehyde and n-acylated cysteines. *J. Chromatogr.* **1989**, *476*, 73–82. [CrossRef]
40. Gord Noshahri, N.; Fooladi, J.; Syldatk, C.; Engel, U.; Heravi, M.M.; Zare Mehrjerdi, M.; Rudat, J. Screening and comparative characterization of microorganisms from Iranian soil samples showing ω-transaminase activity toward a plethora of substrates. *Catalysts* **2019**, *9*, 874. [CrossRef]